

N 7 2 3 3 4 7 9

**NASA TECHNICAL
MEMORANDUM**

NASA TM X-68142

NASA TM X-68142

**CASE FILE
COPY**

**THE APPLICATION OF ELASTOHYDRODYNAMIC
LUBRICATION IN GEAR TOOTH CONTACTS**

by Dennis P. Townsend
Lewis Research Center
Cleveland, Ohio

TECHNICAL PAPER proposed for presentation at
International Lubrication Conference sponsored by the
American Society of Mechanical Engineers and the
American Society of Lubrication Engineers
New York, New York, October 9-13, 1972

THE APPLICATION OF ELASTOHYDRODYNAMIC LUBRICATION
IN GEAR TOOTH CONTACTS

by Dennis P. Townsend

Lewis Research Center

ABSTRACT

Gear lubricants prevent failure under several regimes of operation, such as boundary lubrication, mixed lubrication, and full elastohydrodynamic (EHD) film operation. Gears operating under boundary and mixed lubrication require added protection by using extreme pressure (EP) and anti-wear additive to prevent failure. Understanding the mechanism of how these additives work can aid the designer in his selection of a lubricant for a particular gear application. In many applications gears operate with a full EHD film. The method of EHD film formation and how the lubricant properties affects gear failure and life. The practical aspects of gear lubrication is presented such as the mechanical and service variables which must be considered to obtain optimum gear performance under severe operating conditions.

NOMENCLATURE

- b Hertzian half width, in.
- C center distance, in.
- D_o outside diameter of gear, in.
- D_b base diameter of gear, in.
- d_b base diameter of pinion, in.
- d_o outside diameter of pinion, in.

E	elastic modulus, lb/in. ²
E'	equivalent elastic modulus, lb/in. ²
e	exponent, 2.718
G	dimensionless material parameter, $\alpha E'$
H _{min}	dimensionless film parameter, h/R
h _{min}	EHD film thickness, in. or μ in.
n	exponent of h for fatigue life
P	pressure in contact zone, lb/in. ²
Q _m	speed factor
R	equivalent radius, in.
R _{1, 2}	radius of contacting rollers, in.
U	dimensionless speed parameter, $\mu_0(U_1 + U_2)E'R$
U _{1, 2}	tangential velocity of rolling contact, in./sec
W	dimensionless load parameter, W'/E'R
W'	load per unit width, lb/in.
X	distance along the line of action, in.
Z	length of line of action, in.
α	pressure viscosity coefficient, in. ² /lb
β	ratio of central film thickness
δ	Poisson ratio
θ	gear pressure angle, deg
Λ	EHD film to roughness parameter
μ	lubricant viscosity at contact pressure, lb-sec/in. ²
μ_0	lubricant viscosity at atmospheric pressure, lb-sec/in. ²
ν	lubricant viscosities, centistokes
ρ	density, g/cc

σ	composite surface roughness, rms μ in.
$\sigma_{1,2}$	surface roughness of contacting surfaces, rms μ in.
φ_T	film thickness reduction factor
ω	rotational speed, rad/sec
ψ	inlet boundary

INTRODUCTION

Gear lubrication is a complex problem involving many technical areas. These include fluid hydrodynamics, materials, lubricant technology, metrology, surface chemistry, heat transfer, and kinematics. Gears may fail from many causes such as tooth fracture, scoring, pitting, and wear. Conditions under which these failures occur are shown in figure 1 (ref. 1). Pitting is normally a long-life type failure while wear and scoring may be causes of early failures from a variety of reasons. For a gear system to operate for a long life without wear or scoring and other surface-type failures, it must be lubricated in a way that will prevent the occurrence of more than a slight amount of metal to metal contact. This type lubrication, which prevents or minimizes surface asperity interaction is referred to as elastohydrodynamic lubrication. This lubrication mode is differentiated from boundary lubrication which comprises essentially metal to metal contact with a chemical or oxide film preventing gross wear or welding of the asperities. In most gear applications a combination of elastohydrodynamic and boundary lubrication exists. This paper essentially outlines and defines those parameters which affect the lubrication of gears including surface finish, tooth design, lubricant type, and elastohydrodynamic lubrication principles.

ELASTOHYDRODYNAMIC LUBRICATION

Elastohydrodynamic lubrication combines the hydrodynamic properties of the lubricant with the elastic properties of the material. These factors

combine to form a thin film of lubricant several microinches thick between two contacting surfaces such as bearing or gears even under very high loads.

When two curved surfaces in a gear come into contact with a lubricant film on one or both surfaces, the surfaces are elastically deformed and the contact pressure increases the lubricant viscosity by several orders of magnitude. This increase in viscosity prevents the lubricant from being squeezed out of the contact area and also prevents the surfaces from coming together. An example of the increase in viscosity with pressure is shown in figure 2 (ref. 2) which is a plot of pressure versus viscosity for a synthetic lubricant diester, di (2-ethyl-hexyl) sebacate. As the fluid is subjected to pressures of 150 000 psi at 77° F the viscosity increases from 18 centipoise at atmospheric pressure to 400 000 centipoise at 150 000 psi.

The fluid at this extremely high viscosity resists being squeezed out of the contact zone, and the load is thus transmitted from one element through the lubricant film to the other element. In fact, it can be, and has been, shown that a steel ball can be loaded against a bearing groove with 200 000 psi maximum Hertz stress (i.e., the maximum contact pressure) and with a lubricant film on the groove, the surfaces will remain separated for several hours. Figure 3 (ref. 3) is a cross section through the film of a ball loaded against a flat plate and shows how the pressure-viscosity effects increase the film thickness in the higher pressure region near the center of the contact zone.

Several people have measured the EHD film thickness between rolling disks and between a ball and disk by at least four different methods. Sibley et al. (ref. 4), at the Battelle Columbus Laboratories, have measured the EHD film thickness between rolling disks using X-ray techniques. Figure 4 is a view of the X-ray disk apparatus used at Battelle. Here an X-ray source is collimated into a beam which is passed through the contact zone. A Geiger counter on the other side of the contact zone measures the intensity of the X-ray which determines the film thickness. Figure 5 is a film thickness measurement along the axial direction. Film thickness can also be taken in the circumferential direction. Battelle has also measured the film pressures and temperatures using

thin film transducers on the surface of the disk. Film thickness at much higher loads was also measured and was found to have a greater dependence on load than that previously observed at the lighter loads (ref. 5). The data are shown in figure 6. It should be pointed out that the X-ray method measures minimum film thickness and must be carefully calibrated to obtain accurate results.

Crook (ref. 6) first measured film thickness of the EHD oil film indirectly by measuring the capacitance between the disk at the outlet of the contact and a trailing pad which assumes the thickness measured is one-half the EHD film thickness.

Dyson (ref. 7) measured the capacitance between two disks directly to obtain the EHD film thickness. Dyson measured the film thickness of several lubricants with pure rolling and with rolling and sliding. Figure 7 is a typical curve obtained by Dyson where he compares the calculated film thickness with the measured film thickness. As can be seen, the measured film thickness compares favorably with the calculated film thickness except at the larger film thickness, where it departs slightly because it is becoming more hydrodynamic than EHD. It is interesting to note here that the film thickness with pure rolling and that with rolling and sliding are identical, which indicates that sliding may have no influence on the EHD film thickness. This is predicted by theory which says the film thickness is dependent on the inlet viscosity only. Crook has shown this, as can be seen in figure 8 (ref. 6), where the introduction of severe sliding at constant sum velocities and inlet viscosity reduced the viscosities in the contact zone from 600 poise to 14 poise, while the film thickness fell only 10 percent. The capacitance method measures the average capacitance of the EHD film plus the surrounding capacitance. Some error could therefore be expected for minimum film thickness unless corrected for especially at very thin films. Also, the dielectric properties of the fluids must be known.

SKF Industries under contract to NASA has measured film thickness in bearings using the capacitance method and an electrical conductivity method developed by SKF. With this method, a 400-cycle mv potential is impressed across the bearing races, and the number of asperity contacts is measured. Using the

data obtained and a calibration curve obtained analytically using a random gaussian process to describe the surface, the film thickness can be determined over a limited range. This range is an h/σ of approximately 1.5 to 4. When the capacitance method is used, it will not measure very accurately below the film thickness where asperities began to touch since at this point it begins to short the capacitance. Below this point, which is an h/σ of approximately 4, the conductivity method measures the film thickness. Figure 9 is a photograph of the oscilloscope trace of the conductivity method. Here one can see the 400-cycle voltage; the vertical lines or spikes on this trace are asperity contacts. This particular trace represents a film parameter h/σ of approximately 3.5. Figure 10 shows a similar trace with an h/σ of approximately 2.5. The accuracy of the resistance method is dependent on how well the surface roughness can be represented analytically and how accurately the measuring system can be calibrated to the analytical representation of surface roughness.

Another one of the very interesting methods of measuring EHD film thickness is the optical method developed by Dr. A. Cameron at Imperial College, London (ref. 3). Figure 11 shows how this device works. Light is passed through a glass or other transparent material such as sapphire and is reflected from the contact zone into a lens system in the form of newton rings which give a measure of the film thickness at the contact zone of the rotating ball and transparent plate. Figure 12 is a photograph of the image seen through the eyepiece. The film thickness is measured by watching the contact zone from startup and counting the number of rings as the film thickness increases. The variation in film thickness can be seen in the figure. The minimum film thickness occurs at the sides of the contact, where side leakage and low pressure reduces the film thickness. The trailing edge is also somewhat thinner than the center region of the contact zone because of oil starvation and/or leakage at the contact outlet. Figure 13 is a profile in two directions of the film thickness measured by the optical method. It can be seen that the film thickness at the sides is approximately half that in the center of the contact zone and the side film thickness is much more sensitive to load. In line contact the side effect does not seem to be as severe while the exit film thickness is reduced approximately 20 percent. The accuracy of the optical method

should be very good provided the spacing between lines can be accurately determined. This spacing depends on the refractive index of the coated glass and the refractive index of the oils plus ones ability to measure the fringes accurately. Then the deflection of the ball is different from the glass or sapphire.

Although considerable research has been applied to EHD technology, there is still much to learn. Specifically, more information is needed on the properties of the fluid as it undergoes rapid changes in pressure, temperature, and shear rate. Also, a better understanding is needed on the thermal conditions existing in the films and surfaces during rolling and sliding conditions.

In order to determine the EHD film thickness by using existing theories, the temperature of the lubricants entering the contact zone must be known. This temperature is practically identical to the temperature of the metal surface on which it lies except at high-rolling speeds where Cheng (ref. 8) and Greenwood et al. (ref. 9) have shown that heating of the lubricant occurs at the inlet to the EHD contact zone. If this temperature of the metal is to be known, it must either be measured or calculated from the traction force in the contact zone. This traction force is not the same as a coefficient of friction because the force changes over the width of the contact zone and is dependent on the lubricant viscosity. As the contact zone undergoes sliding and increased temperatures, the viscosity changes considerably. The temperature and shear rate reduce the viscosity at pressure. If the viscosity followed an exponential increase, the lubricant would become stronger than the bearing metal.

H. Naylor (ref. 10) presented a plot of friction against sliding speed (fig. 14) to show how the friction changes with increased sliding speed and possible causes for this change. In work conducted at NASA (ref. 11) the traction in a spinning contact of a ball in a lubricated groove was measured and an analysis conducted to calculate the traction force in the spinning contact zone. In the analysis, the curve shown in figure 15 was used with the pressure-viscosity equation as shown. When this equation was used, the analysis matched the experimental analysis, as shown in figure 16. Tests were also conducted at NASA Lewis Research Center (ref. 12) to determine what effect several additives would have on the

traction forces in a spinning EHD contact. As can be seen from figure 17, the effects of different concentrations of several additives in a synthetic paraffinic oil had no effect on the traction force, even with a film thickness that could be considered in the regime where asperity interaction would occur. The implications from these data are that the additive used here does not affect the traction force in the contact zone and does not change the rheological properties of the lubricant. Workers at MTI have generated a set of curves for the friction coefficient based on three parameters as G_1 , G_2 , and G_3 (ref. 13). G_1 is the shear rate parameter and G_2 and G_3 are the thermo heating and pressure viscosity parameters, respectively. These curves are contained in reference 13.

ELASTOHYDRODYNAMIC THEORY

Formation of a lubricant film between rolling elements such as gears and bearings results from the elastic deformation of the surfaces and the hydrodynamic action of the lubricant. The flattening of the surfaces spreads the load and reduces the contact pressure while the viscous drag and rolling action can draw the lubricant into the contact area (ref. 14). As the lubricant enters the contact zone, it undergoes a pressure rise. The pressure rise sharply increases the lubricant viscosity to a very high value and prevents the lubricant from being squeezed from between the surfaces. The increase of viscosity with pressure is commonly represented as

$$\mu = \mu_0 e^{\alpha p} \quad (1)$$

Pressure does not affect the atmospheric viscosity μ_0 nor the pressure-viscosity coefficient α .

A. N. Grubin in 1949 developed an approximate film-thickness equation for highly loaded elastic contacts which allowed for the effect of pressure on viscosity (ref. 15). The Grubin model of an EHD lubricated contact is shown in figure 18.

Grubin's model simplifies the EHD lubrication problem by considering long cylinders and thus disregarding variations in the axial direction. Also, the model assumes that deflections of the contacting surfaces, specifically in the inlet region, are the same under elastohydrodynamic conditions as they would be in static dry contact. The solution for film thickness is thus based on a Hertzian shape for the deformed cylinders, in the inlet region, and can be expressed as:

$$\frac{h_{\min}}{R} = 1.6 \frac{(\alpha E')^{0.6}}{\left(\frac{W'}{E'R}\right)^{0.13}} \left[\frac{\mu_0(V_1 + V_2)}{E'R} \right]^{0.7} \quad (2)$$

Since the inlet viscosity and the pressure viscosity coefficient are both reduced by increased temperature, it is very important to use the correct temperature of the lubricant when calculating the EHD film thickness. Since the lubricant temperature entering the contact zone is practically identical to the metal temperature regardless of the bulk of oil temperature, the metal temperature should either be measured or calculated.

A simplified dimensionless approximation of equation (2) from reference 15 is

$$H_{\min} = 1.6 \frac{G^{0.6} U^{0.7}}{W^{0.13}} \quad (3)$$

where H_{\min} is the dimensionless film thickness, equal to h_{\min}/R ; G is the materials parameter, equal to $\alpha E'$; W is the load parameter, equal to $W'/E'R$; and W' is the applied tooth load in pounds per inches of tooth width. The speed parameter U is

$$U = \frac{\mu_0(V_1 + V_2)}{E'R}$$

The elastic properties of an equivalent cylinder E' are

$$\frac{1}{E'} = \frac{1}{2} \left[\left(\frac{1 - \delta_1^2}{E_1} \right) + \left(\frac{1 - \delta_2^2}{E_2} \right) \right]$$

For typical steels, E' is 33×10^6 and, for mineral oils, a typical value of α is 1.5×10^{-4} in.²/lb. Thus, for mineral-oil-lubricated rolling elements, $G = 5000$. From figure 19, values of H_{\min} and h_{\min} can be obtained for combinations of G , U , and W . D. Dawson further modified this for line contact (ref. 15) as follows

$$H_{\min} = 2.65 \frac{U^{0.70} G^{0.54}}{W^{0.13}}$$

H. S. Cheng (ref. 8) has developed a method for improving the EHD film thickness calculations for high speeds. He has shown that at higher speeds heating of the lubricant occurs at the inlet region and can considerably reduce the EHD film thickness. Figure 20 is a plot of the film reduction factor φ_T versus the speed factors Q_m . It is readily seen that the film is considerably reduced for the speed factors above 0.1.

Contact geometry of gears and cams can be represented by two contacting cylinders. The geometric similarity outside the contact zone is not of importance.

When using contacting cylinders to approximate the contact of machine elements, it is useful to introduce the concept of an equivalent cylinder. It is assumed the undeformed cylinders are separated by a minimum film thickness h_{\min} (fig. 21(a)). A cylinder with equivalent radius R and with the same minimum film thickness is shown in figure 21(b). The equivalent radius is

$$R = \frac{R_1 R_2}{R_1 + R_2} \quad (4)$$

If R_1 and R_2 lie on the same side of the common tangent, then

$$R = \frac{R_1 R_2}{R_1 - R_2} \quad (5)$$

The tangential velocities are

$$U_1 = \omega_1 R_1 \quad (6)$$

$$U_2 = \omega_2 R_2 \quad (7)$$

The geometry of an involute gear contact is shown in figure 22. Contact at distance X from the pitch point can be represented by two cylinders rotating at the angular velocity of the wheels. Equivalent radius, from equation (4), is

$$R = \frac{(R_1 \sin \theta + X)(R_2 \sin \theta - X)}{(R_1 + R_2) \sin \theta} \quad (8)$$

Contact speeds from equation (6) are

$$U_1 = (R_1 \sin \theta + X)\omega_1 \quad (9)$$

$$U_2 = (R_2 \sin \theta - X)\omega_2 \quad (10)$$

An example of utilizing the above analysis for a simple case of two rolling disk using the Dawson EHD formula is as follows.

Find the film thickness between two steel rollers 1/4-inch wide, diameters of 3 and 2 inches with a load of 500 pounds using Mil-L-7808 lubricant at 210° F. The smaller roller speed is 2000 rpm with no slip between rollers. For this lubricant $\alpha = 0.40 \times 10^{-4}$ in.²/lb and we will use equation (2).

$$\frac{h_{\min}}{R} = 1.6 \frac{(\alpha E')^{0.6}}{\left(\frac{W'}{E'R}\right)^{0.13}} \left[\frac{\mu_0 (V_1 + V_2)}{E'R} \right]^{0.7} \quad (2)$$

$$W' = \frac{P}{L} = \frac{500}{0.25} = 2000 \text{ lb/in.}$$

$$\frac{1}{E'} = \frac{1}{2} \left(\frac{1 - 0.09}{30 \times 10^6} + \frac{1 - 0.09}{30 \times 10^6} \right)$$

$$E' = 33 \times 10^6$$

$\nu = 3.3$ centistokes for Mil-L-7808 at 210°F

$$\mu_0 = \nu \rho \cdot 1.45 \times 10^{-7} = 3.3 \times 0.915 \times 1.45 \times 10^{-7}$$

$$\mu_0 = 4.38 \times 10^{-7} \text{ lb-sec/in.}^2$$

$$R = \frac{R_1 R_2}{R_1 + R_2} = \frac{1.5 \times 1}{2.5} = 0.6 \text{ in.}$$

$$U_1 = U_2 = \frac{\pi R N}{30} = \frac{\pi \times 1 \times 2000}{30} = 210 \text{ in./sec}$$

$$\frac{h_{\min}}{R} = \frac{1.6(0.40 \times 10^{-4} \times 33 \times 10^6)^{0.6}}{(2000/33 \times 10^6 \times 0.6)^{0.13}} \left[\frac{4.38 \times 10^{-7} (420)}{33 \times 10^6 \times 0.6} \right]^{0.7}$$

$$\frac{h_{\min}}{R} = 7.0 \times 10^{-6} \quad h_{\min} = 4.2 \times 10^{-6} \text{ in.}$$

Using the film reduction factors from reference 8 $Q_m = 0.003$ and $\varphi_1 = 1$, therefore, h_{\min} remains unchanged for this low speed case.

HOW THICK A FILM?

Surface topography is important to the EHD lubrication process. EHD theory is based on the assumption of perfectly smooth surfaces, that is, no interaction of surface asperities. Actually, of course, this

is not the case. An EHD film of several millionths of an inch can be considered adequate for highly loaded rolling elements in a high-temperature environment. However, the calculated film might be less than the combined surface roughness of the contacting elements. If this condition exists, surface asperity contact, surface distress (in the form of surface glazing and pitting), and surface smearing or deformation can occur. Extended operation under these conditions can result in high wear, excessive vibration, and seizure of mating components. A surface-roughness criterion for determining the extent of asperity contact is based upon the ratio of film thickness to a composite surface roughness. The film parameter Λ is

$$\Lambda = \frac{h_{\min}}{\sigma} \quad (11)$$

where composite roughness σ is

$$\sigma = (\sigma_1^2 + \sigma_2^2)^{1/2} \quad (12)$$

and σ_1 and σ_2 are the rms roughness of the two surfaces in contact. Figure 23 is a plot, based upon experimental data, of percent of complete asperity or surface separation (percent film) as a function of film parameter Λ . At values of less than 1, surface smearing or deformation, accompanied by wear, will occur (fig. 24(d)). When Λ is between 1 and 1.5, surface distress such as shown in figure 24(c) can occur. For values between 1.5 and 3 some surface glazing occurs (fig. 24(b)). At values of 3 or greater, minimal wear can be expected with the resulting surface appearance illustrated in figure 24(a). These figures are those of bearing inner races.

PRACTICAL ASPECTS OF LUBRICATION

Even though a theoretical EHD film thickness is calculated for a particular application the design may still experience failure problems such as wear, scoring or pitting of the gear surfaces. In present day gearing,

scoring is the predominate mode of failure and is the result of a breakdown in the lubricant and/or boundary film separating the load carrying members. The function of the gear lubricant is to cool the gear surfaces and provide a film of lubricant that prevents metal to metal contact which would result in wear or scoring.

There are many factors that can affect the start of scoring. Some of these factors which affect scoring are shown in figures 25 to 27 (ref. 17). Figure 25 shows the effect of surface finish on scoring where the load capacity at 20 microinches rms is approximately twice the load capacity at 60 microinches rms. For the example shown, increased surface roughness above about 60 microinches rms does not seem to reduce load-carrying capacity appreciably. Others have shown similar results (ref. 18).

Figure 26 shows how tip relief can improve the scoring load capacity of a set of gears. In this case, tip relief up to 0.0008 was effective in improving load capacity, but beyond 0.0008 the load capacity was reduced. Tip relief is effective because it corrects for tooth deflection that would cause the gear teeth to contact unevenly or incorrectly. Other mechanical factors such as alignment and diametral pitch can have an effect on the scoring load. Several operating factors can also have an effect on load capacity. These are speed, temperature, and viscosity of the lubricant as well as the type of additive present in the lubricant.

A notable effect on the load-carrying capacity of gears is the method of applying the lubricant to the gear, as shown in figure 27 (ref. 17). Here 0° represents the gears coming into mesh and 360° , the gears going out of mesh. As can be seen, the load capacity is affected by the jet velocity and by the jet location. The jet velocity can affect how much oil strikes the tooth as well as the cooling rate of the lubricant. Usually the best cooling of the gear tooth surface is obtained by jet application at the gear outlet and best lubrication at the gear inlet. Cooling of the gear tooth surface is very important in improving load carrying capacity. In large high-speed gears, more than one oil jet may be required to adequately cool the gear surfaces since most of the lubricant supplied by each jet is thrown off without affecting the cooling of the surface.

In wide gears operating at high speeds considerable power can be lost by applying jet lubricant to the inlet mesh because the gears will trap the lubricants between the gear teeth as shown in figure 28. In such cases, a fine mist spray or low oil flow jet would best serve to apply lubricant to the gear teeth at the inlet mesh. Mist lubrication can supply adequate lubricant to the surfaces but will not supply adequate cooling in most cases.

In jet cooling of the gear teeth, it is also important that the jet of lubricant have sufficient velocity and be in the proper direction so that it will strike the tooth surface that should be cooled, figure 28 (ref. 19). The amount of lubricant remaining on the tooth as it approaches the inlet mesh is a function of the viscosity, which is a function of temperature; this indicates that cooling on the outlet mesh will help the lubricant film at the inlet mesh.

Generous amounts of oil may be supplied to a bearing or gear and still not provide a good oil film at the load carrying surfaces. Oil starvation can cause a reduction in the EHD film thickness as shown in figure 29 (ref. 20). This curve implies that at some conditions of starvation the film will be thinner than calculated. However, it is difficult, if not impossible, to determine what amount of starvation might occur under any given condition. In high-speed bearings, starvation might occur because the lubricant does not enter the bearing but is thrown off before it can accomplish its intended purpose of lubricating the rolling-element surfaces. In gearing, the lubricant can be flung off and leave an insufficient film remaining for proper lubrication.

BOUNDARY LUBRICATION

Extreme-pressure lubricants can significantly increase the load carrying capacity of gears. The extreme-pressure additives in the lubricating fluid form a film on the surfaces by chemical reaction, adsorption, and/or chemisorption. These boundary films can be less than 1 microinch to several microinches thick (ref. 22). These films may appear as shown in figure 30 (ref. 21) for the chemical reaction of sulfur and in

figure 31 for the chemisorption of iron stearate. Figure 32 shows the range of film thicknesses for various films (ref. 22). The films can provide separation of the metal surfaces when the lubricant becomes thin enough for the asperities to interact. The boundary film probably provides lubrication by microasperity-elastohydrodynamic lubrication (ref. 22), as shown in figure 33; here the asperities deform under the load. The boundary film prevents contact of the asperities and at the same time provides low shear strength properties that prevent shearing of the metal and reduce the friction coefficient over that of the base metal. These boundary films provide lubrication at different temperature conditions, depending on the materials used. For example, some boundary films will melt at a lower temperature than others, as can be seen in figure 34 (ref. 21), and will then fail to provide protection of the surfaces. The "failure temperature" is the temperature at which the lubricant film fails. In extreme-pressure lubrication this failure temperature is the temperature at which the boundary film melts. The melting point or thermal stability of surface films appears to be one unifying physical property governing failure temperature for a wide range of materials (ref. 21). It is based on the observation (ref. 24) that only a film which is solid can properly interfere with potential asperity contacts. For this reason, many extreme-pressure lubricants contain more than one chemical for protection over a wide temperature range. For instance, Borsoff (refs. 25 and 26) found that phosphorus compounds were superior to chlorine and sulfur at slow speeds, while sulfur was superior at high speeds. He explains this as a result of the increased surface temperature at the higher speeds. It should be remembered that most extreme-pressure additives are chemically reactive and increase their chemical activity as temperature is increased. Horlick (ref. 27) found that some metals such as zinc and copper had to be removed from their systems when using certain extreme-pressure additives.

EXTREME PRESSURE AND ANTI-WEAR ADDITIVE SELECTION

Some of the extreme-pressure additives commonly used for gear oil are those containing one or more compounds of chlorine, phosphorus,

sulfur or lead soaps (ref. 28). Many chlorine containing compounds have been suggested for extreme-pressure additives but few have actually been used. Some lubricants are made with chlorine containing molecules where the Cl₃-C linkage is used. For example, either tri (trichloroethyl) or tri (trichlorotert butyl) phosphate additives have shown high load carrying capacity. Other chlorine containing additives are chlorinated paraffin or petroleum waxes and hexachlorethane.

The phosphorus containing compounds are perhaps the most commonly used additives for gear oils. Some aircraft lubricants have 3 to 5 percent tricresyl phosphate or tributyl phosphite as either an extreme-pressure or anti-wear agent. Other phosphorus extreme-pressure agents used in percentages of 0.1 to 2.0 percent could be dodecyl dihydrogen phosphate, diethyl-, dibutyl-, or dicresyl- phenyl trichloroethyl phosphite and a phosphate ester containing a pentachlorphenyl radical. Most of the phosphorus compounds in gear oils also have other active elements.

The sulfur containing extreme-pressure additives are believed to form iron sulfide films that prevent wear up to very high loads and speeds. However, they give higher friction coefficients and are, therefore, usually supplemented by other boundary film forming ingredients that reduce friction. The sulfur compounds should have controlled chemical activity (such as oils containing dibenzyl disulfide of 0.1 or more percent). Other sulfur containing extreme-pressure additives are diamyl disulfide, dilauryl disulfide, sulfurized oleic acid and sperm oil mixtures, and dibutylxanthic acid disulfide.

Lead soaps have been used in lubricants for many years. They resist the wiping and sliding action in gears and they help prevent corrosion of steel in the presence of water. Some of the lead soaps used in lubricants are lead oleate, lead fishate, lead-12-hydroxystearate, and lead naphthenate. The lead soap additive most often used is lead naphthenate because of its solubility. Lead soaps are used in concentrations of from 5 to 30 percent.

There are other additive compounds that contain combinations of these elements and most extreme-pressure lubricants contain more than one extreme-pressure additive. Needless to say, the selection of a proper

extreme-pressure additive is a complicated process. The word susceptibility is frequently used with reference to additives in oils to indicate the ability of the oil to accept the additive without deleterious effects. Such things as solubility, volatility, stability, compatibility, load carrying capacity, cost, etc., must be considered.

Many gear oil compounds depend upon the use of proprietary or package extreme-pressure additives. As a result, the lubricant manufacture does not evaluate the additives' effectiveness. Because of this, any selection of extreme-pressure additives should be supported by an evaluation program to determine their effectiveness for a given application. However, a few firms have considerable background in the manufacture and use of extreme-pressure additives for gear lubrication and their recommendations are usually accepted without question by users of gear oils.

Reference 28 lists several representative oil formulations for different applications containing several additives. Table I is a list of three lubricants with additives for hypoid gear operation. Table II is a list of four lead containing extreme-pressure gear oils. The SCL is a compound containing sulfur-chlorine-lead and fatty oil. Table III is a typical formulation for a jet turbine lubricant.

CONTACT PRESSURE - DIFFERENT FROM THEORY

Typical EHD pressure traces in the contact zone, theoretically obtained, are shown in figure 35. The maximum Hertz stress (maximum contact pressure) corresponding to dry contact is shown by the semi-elliptical curve. For a contacting cylinder,

$$S_{\max} = \frac{W^{1/2}}{(2\pi)^{1/2}} E' \quad (13)$$

and

$$b = 2RW^{1/2} \quad (14)$$

where

$$W = \frac{W'}{E'R}$$

An unusual feature of the pressure distributions in the contact zone is the presence of a pressure spike. At low tangential velocities, the spike is near the trailing edge of the contact zone. At higher velocities, it shifts toward the leading edge, and the pressure patterns differ sharply from the Hertz dry-contact pattern.

For those cases corresponding in figures 35(a), (c), and (d), maximum shearing stress is about the same magnitude as for dry contact. The case shown in figure 35(b) has a stress about 15 percent higher than dry contact stress. Also, for cases shown in figures 35(a) and (b), maximum shearing stresses occurred closer to the surface of the contact area.

Experimental work has shown that actual pressure distributions deviate from those predicted from theory. This is illustrated in figure 36 for contacting cylindrical disks at maximum Hertz stresses between 104 000 and 128 000 psi. The pressure curve tends to wrap around the calculated Hertz (dry-contact) stress distribution. The pressure spike tends to move toward the trailing edge. This trend continues for higher contact stresses. However, for these higher stresses, the pressure spike cannot be experimentally detected.

What is significant about the pressure profiles is that the average Hertz stress is decreased from the nonlubricated condition. For similar pressure profiles, a 10-percent decrease in the average stress can mean a 100-percent increase in fatigue life.

ELASTOHYDRODYNAMIC LUBRICATION AND FATIGUE LIFE - STRONG RELATIONSHIP

When a sufficient EHD film is present, gears will have much longer lives and will usually fail from fatigue. Fatigue usually manifests itself, in the early stages, as a shallow spall with a diameter about the same as

the contact width. A fatigue failure for gears is shown in figure 37 (ref. 30). As atmospheric viscosity of a particular lubricant is increased, the fatigue life of the gear or bearing also increases. If the lubricant pressure-viscosity coefficient is increased by changing the lubricant base stock, longer fatigue life can be obtained for a given lubricant at atmospheric conditions. It has become generally accepted that fatigue life increases with increases in viscosity, pressure-viscosity coefficient, or speed. These factors imply increasing fatigue life with increasing EHD film thickness

$$\text{Life} \propto (h_{\min})^n \quad (15)$$

Much experimental work needs to be done to determine the value of the exponent n . However, it appears that an interrelation exists among fatigue life, contact-pressure distribution, and lubricant film thickness.

HOW TO USE EHD THEORY

Using the principles and theory previously discussed, design procedures for EHD application can be outlined. It is important, however, to realize that further refinements of EHD theory are required and are currently being undertaken. It is also very important to use the correct inlet oil temperature, which usually corresponds to the metal temperature. The methods presented do not consider non-Newtonian behavior of the lubricant. This factor probably accounts for the fact that some measurements of EHD film thickness were less than half the value predicted by theory. Thus, these procedures are a guide only, not a guarantee of successful gear or bearing operation. The procedure is

- (1) Determine equivalent radius R , from equation (8).
- (2) Determine contact speed U_1 and U_2 from equations (9) and (10).
- (3) Determine values for G , U , and W from equation (3).
- (4) Calculate the dimensionless film thickness H_{\min} from equation (3) or figure 19.
- (5) Determine the film reduction factor φ_T .

(6) Determine film thickness h_{\min} from equation (2).

(7) Determine surface composite roughness σ from equation (12) and the film parameter from equation (11).

(8) With Λ , determine from figure 23 the percent film. If the percent film is less than 80 percent, which is equivalent to a Λ of 2, changes in one or more of the EHD parameters should be considered to avoid surface distress.

(9) Where Λ is less than 2 and where operating conditions or lubricant cannot be changed, to improve the Λ value, careful consideration must be taken to properly select EP or anti-wear additives to assure long life operation without gross surface distress or wear.

An example of using the analysis for gears as given above is as follows.

Find the film thickness and h/σ at the end point of tooth contact for a set of steel gears running at 5000 rpm with 7808 lubricant at 210° F. Tooth load is 2000 pounds per inch at all points of contact. Pitch diameter 3.5 inches, outside diameter 2.75 inches, diametral pitch 8 and surface finish 12 microinches rms.

$$Z = \frac{(D_o^2 - D_b^2)^{1/2} + (d_o^2 - d_b^2)^{1/2} - 2C \sin \theta}{2}$$

$$D_b = d_b = 3.5 \cos 20^{\circ} = 3.289$$

$$Z = (3.75^2 - 3.289^2)^{1/2} - 3.5 \times 0.342$$

$$Z = 0.6043 \quad X_{\max} = \frac{Z}{2} = 0.30215$$

$$R = \frac{(R_p \sin \theta + X)(R_p \sin \theta - X)}{2R_p \sin \theta}$$

$$R = \frac{(1.75 \times 0.342 + 0.302)(1.75 \times 0.342 - 0.302)}{3.5 \times 0.342} = \frac{0.9 \times 0.3}{1.2}$$

$$R = 0.2255$$

$$U_1 = \omega R_1 \quad U_2 = \omega R_2$$

$$U_1 = \frac{\pi 5000}{30} \times 0.9 = 470 \text{ in./sec}$$

$$U_2 = \frac{\pi 5000}{30} \times 0.3 = 157 \text{ in./sec}$$

$$U_1 + U_2 = 627 \text{ in./sec}$$

$$\frac{h_{\min}}{R} = \frac{1.6(0.4 \times 10^{-4} \times 33 \times 10^6)^{0.6}}{(2000/33 \times 10^6 \times 0.2255)^{0.13}} \left(\frac{4.38 \times 10^{-13} \times 627}{33 \times 10^6 \times 0.2255} \right)^{0.7}$$

$$\frac{h_{\min}}{R} = 17.3 \times 10^{-6}$$

$$Q_m = 0.006 \quad \text{and} \quad \varphi_T = 1$$

$$h_{\min} = 4 \times 10^{-6}$$

$$\sigma = (12^2 + 12^2)^{1/2} = 17$$

$$\Lambda = \frac{h}{\sigma} = \frac{4}{17} = 0.24$$

CONCLUDING REMARKS

The main function in the lubrication of gearing is to prevent the scoring and fatigue failure of the gear contact surfaces. Much can be done in the early stages of design of gear systems to accomplish these goals.

1. The designer should consider tip relief as an aid to improving load capacity.
 2. He should also weigh the cost of improved surface finish for better load capacity against other factors.
 3. In gear applications requiring high speed and/or loads, special care should be given to the location and application of the lubricant for best results.
 4. An analysis should be conducted to determine the EHD film thickness with care given to the worst operating conditions of temperature, speed, and load. This analysis will aid in the selection of the lubricant that will give best results. It should also tell the designer if an extreme pressure additive is needed to prevent scoring. Many times a startup or shutdown condition may require the use of an additive.
 5. In selecting an extreme pressure additive the designer should be aware of the temperature, speed, and loads expected in the system.
 6. Finally, because there is much that still is unknown about the lubrication of concentrated contacts, a test program should be included in any new transmission or gear box design to assure successful operation of the system.
- #### REFERENCES
1. Wellauer, E. S., Discussion at the University of Wisconsin Gear Design Seminar. Nov. 1968 (unpublished).
 2. Research Committee on Lubrication, "Viscosity and Density of Over 40 Fluids at Pressures to 152,000 psi and Temperatures to 425° F," ASME, New York, 1953.
 3. Foord, C. A., Hammann, W. C., and Cameron, A., "Evaluation of Lubricants Using Optical Elastohydrodynamics," ASLE Transactions, Vol. 11, No. 1, Jan. 1968, pp. 31-43.
 4. Sibley, L. B., and Orcutt, F. K., "Elasto-Hydrodynamic Lubrication of Rolling-Contact Surfaces," ASLE Transactions, Vol. 4, No. 2, Nov. 1961, pp. 234-249.

5. Parker, R. J., and Kannel, J. W., "Elastohydrodynamic Film Thickness Between Rolling Disks with a Synthetic Paraffinic Oil to 589° K (100° F)," TN D-6411, 1971, NASA, Cleveland, Ohio.
6. Crook, A. W., "The Lubrication of Rollers," Philosophical Transactions of the Royal Society of London, Ser. A, Vol. 250, no. 981, Jan. 23, 1958, pp. 387-409.
7. Dyson, A., Naylor, H., and Wilson, A. R., "The Measurement of Oil-Film Thickness in Elastohydrodynamic Contacts," Elastohydrodynamic Lubrication, Proceedings of the Institutional Mechanical Engineers, Vol. 180, Pt. 3B, 1965.
8. Cheng, H. S., "Calculation of Elastohydrodynamic Film Thickness in High-Speed Rolling and Sliding Contacts," MTI-67TR24, AD-652924, May 1967, Mechanical Technology, Inc., Latham, N. Y.
9. Greenneed, J. A., and Kauzlarich, J. J., "Inlet Shear Heating in Elastohydrodynamic Lubrication," University of Virginia for NASA Grant.
10. Naylor, H., "The Rheological Behavior of Lubricants," Interdisciplinary Approach to the Lubrication of Concentrated Contacts, SP-237, 1970, NASA, Washington, D.C., pp. 279-307.
11. Allen, C. W., Townsend, D. P., and Zaretsky, E. V., "Elastohydrodynamic Lubrication of a Spinning Ball in a Nonconforming Groove," Journal of Lubrication Technology, Vol. 92, No. 1, Jan. 1970, pp. 89-96.
12. Townsend, D. P., and Zaretsky, E. V., "Effects of Antiwear and Extreme-Pressure Additives in a Synthetic Paraffinic Lubricant on Ball Spinning Torque," TN D-5820, 1970, NASA, Cleveland, Ohio.
13. McGrew, J. M., Gu, A., Cheng, H. S., and Murray, S. F., "Elastohydrodynamic Lubrication: Preliminary Design Manual," AFAPL-TR-70-27, Nov. 1970, Mechanical Technology, Inc., Latham, N. Y.

14. Zaretsky, E. V., and Anderson, W. J., "How to Use What We Know About EHD Lubrication," Machine Design, Vol. 40, No. 26, Nov. 7, 1968, pp. 167-173.
15. Grubin, A. N., and Venogradov, I. E., "Investigation of the Contact of Machine Components," Book 30, 1949, Central Scientific Research Institute for Technology and Mechanical Engineering (TSNI TMASH), Moscow.
16. Dowson, D., and Higginson, G. R., Elastohydrodynamic Lubrication, Pergamon Press, Ltd, 1966.
17. Borsoff, V. N.: On the Mechanism of Gear Lubrication. J. Basic Eng., vol. 81, no. 1, Mar. 1959, pp. 79-93.
18. Seireg, A., and Conry, T., "Optimum Design of Gear Systems for Surface Durability," ASLE Transactions, Vol. 11, No. 4, Oct. 1968, pp. 321-329.
19. McCain, J. W., and Alsandor, E., "Analytical Aspects of Gear Lubrication on the Disengaging Side," ASLE Transactions, Vol. 9, No. 2, Apr. 1966, pp. 202-211.
20. Wolveridge, P. E., Baglin, K. P., and Archard, J. F., "The Starved Lubrication of Cylinders in Line Contact," Proceedings of the Institution of Mechanical Engineers, Vol. 185, No. 81/71, 1970-71, pp. 1159-1169.
21. Godfrey, D., "Boundary Lubrication," Interdisciplinary Approach to Friction and Wear, SP-181, 1968, NASA, Washington, D.C., pp. 335-384.
22. Fein, R. S., "Chemistry in Concentrated-Conjunction Lubrication," Interdisciplinary Approach to the Lubrication of Concentrated Contacts, SP-237, 1970, NASA, Washington, D.C., pp. 489-527.
23. Fein, R. S., and Kreutz, K. L.: Discussion to Reference 21, pp. 358-376.
24. Bowden, F. P., and Tabor, D., The Friction and Lubrication of Solids, Vol. 2, Clarendon Press, Oxford, 1964, p. 365.

25. Borsoff, V. N., "Fundamentals of Gear Lubrication," Annual Rep., June 1955, Shell Development Co., Emeryville, Calif. (Work under Contract NOa(s) 53-356-c).
26. Borsoff, V. N., and Lulwack, R., "Fundamentals of Gear Lubrication," Final Rep., June 1957, Shell Development Co., Emeryville, Calif. (Work under Contract NOa(s) 53-356-c).
27. Horlick, E. J., and O'D. Thomas, D. E., "Recent Experiences in the Lubrication of Naval Gearing," Gear Lubrication Symposium, Institute of Petroleum, 1966.
28. Boner, C. J., Gear and Transmission Lubricant, Reinhold Pub. Co., New York, 1964.
29. Bell, J. C., and Kannel, J. W., "Aspects of Lubrication Affecting Life of Rolling Bearings," Metals Engineering Quarterly, Vol. 7, no. 1, Feb. 1967, pp. 28-35.
30. Shipley, E. E., "Gear Failure," Machine Design, Vol. 39, No. 28, Dec. 7, 1969, pp. 152-162.

TABLE I. - GEAR OIL FORMULATIONS WHICH SATISFY
 CONDITIONS OF HIGH-SPEED, LOW-TORQUE AND
 LOW-SPEED, HIGH-TORQUE (REF. 28)

	wt %	wt %	wt %
Solvent B. S. vis. 600 Redwood I at 140° F	58.0	-----	-----
Solvent oil-150 Redwood I at 140° F	25.0	-----	-----
Solvent oil-65 Redwood I at 140° F	8.0	-----	-----
Chlorinated paraffin wax-40% Cl	3.7	-----	-----
Dibenzyl disulfide	2.8	-----	-----
Di-isopropyl phosphite	1.4	-----	-----
Oil concentrate 85% of zinc salts of dihexyl and di-isopropyl phosphorodithioic acids	.5	-----	-----
Oil concentrate 40% basic calcium petroleum sulfonate	.5	-----	-----
Polymethacrylate type pour depressant	.1	-----	-----
Additive A	-----	6.9	-----
Zinc dihexyl dithiophosphate	-----	5.5	-----
Oil, 90 V.I., 1094 vis. SUS at 100° F	-----	87.6	-----
Zinc di-(4-methyl-2-pentyl) phosphorodithioate	-----	-----	4.4
Di-benzyl polysulfides	-----	-----	2.05
SAE 90 grade gear oil	-----	-----	93.55

TABLE II. - EP GEAR OILS CONTAINING
LEAD COMPOUNDS (REF. 28)

Composition	A	B	C	D
	Percent by weight			
Lead naphthenate	8	7	-----	-----
Sulfo-chlorinated sperm oil	8	-----	-----	-----
Chlorinated paraffin wax	2.5	-----	-----	-----
Sulfurized sperm oil	4	3	-----	-----
"SCL"	-----	-----	28.5	28.5
Diphenylamine	-----	.3	-----	-----
SAE 90 grade oil	77.5	-----	-----	-----
500 at 100 solvent oil	-----	23.0	-----	-----
200 solvent bright stock	-----	66.7	-----	41.5
200 at 210 black oil	-----	-----	46.0	-----
100 at 100 Arkansas oil	-----	-----	25.5	-----
400 at 100 solvent oil	-----	-----	-----	30.0

TABLE III. - TURBOJET LUBRICANT (REF. 28)

Ingredient	Purpose	Percent
Dodecylamine dodecyl acid phosphate	EP agent	0.12
Dodecyl di-hydrogen phosphate	EP agent	.08
Tricresyl phosphate	Anti-wear agent	2.0
Phenyl alpha naphthylamine	Oxidation inhibitor	1.0
Quinizarin	Metal deactivator	.02
Dimethyl silicon	Anti-foam agent	.001
Fluid		96.78

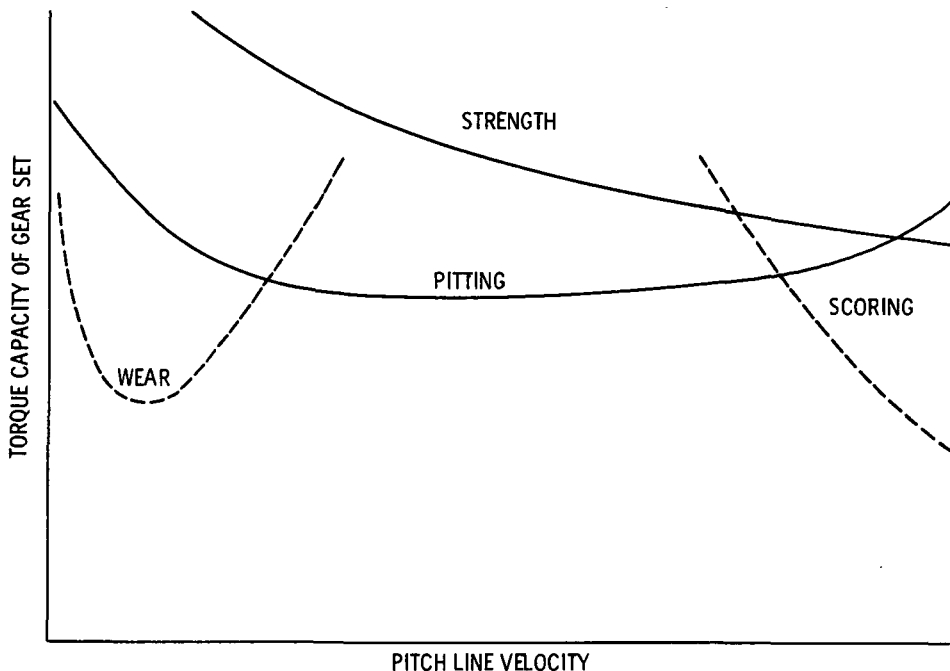


Figure 1. - Probable type of gear distress depends upon pitch line velocity, reference 1.

E-7146

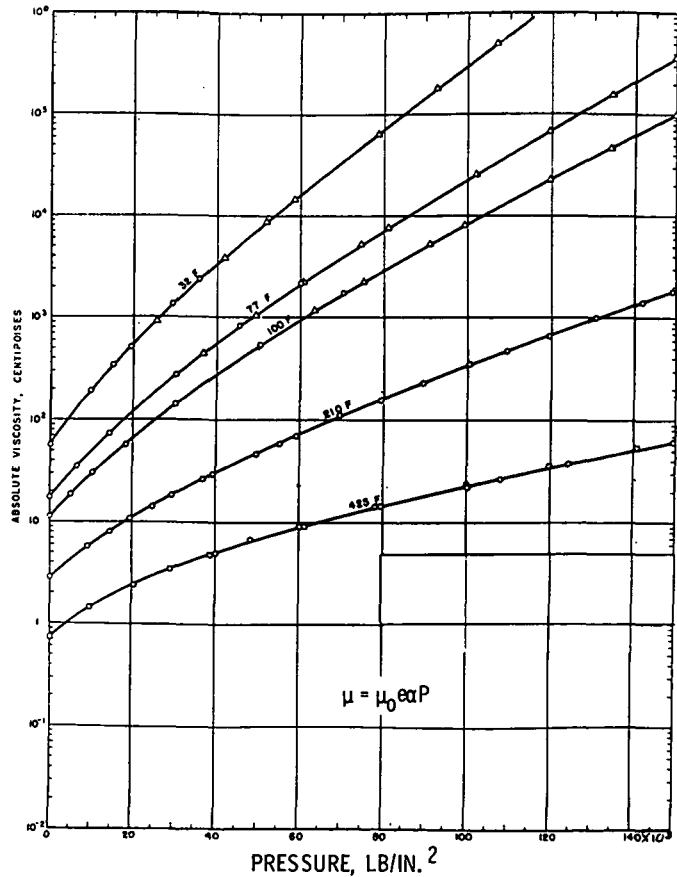


Figure 2. - Pressure viscosity for a synthetic lubricant diester Di- (2 Di- (2-ethyl-hexyl) sebacate, reference 2.

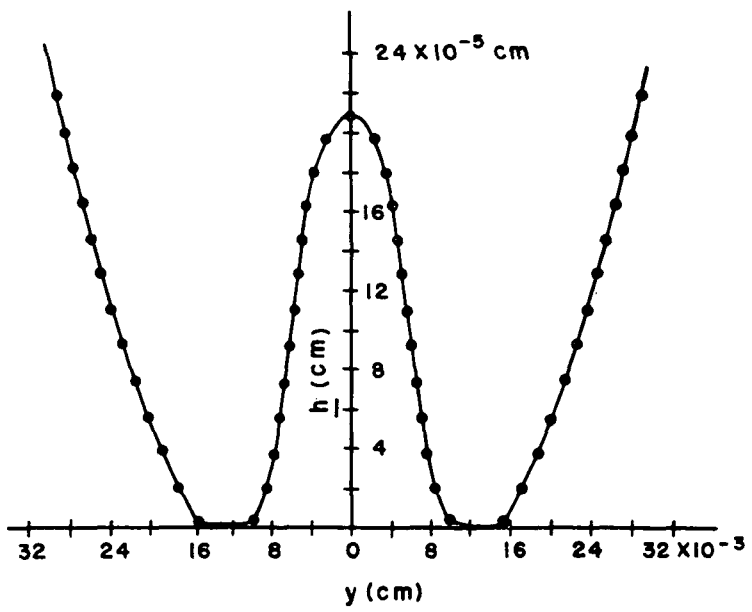


Figure 3. - Cross section through a squeeze film dimple (ref. 3).

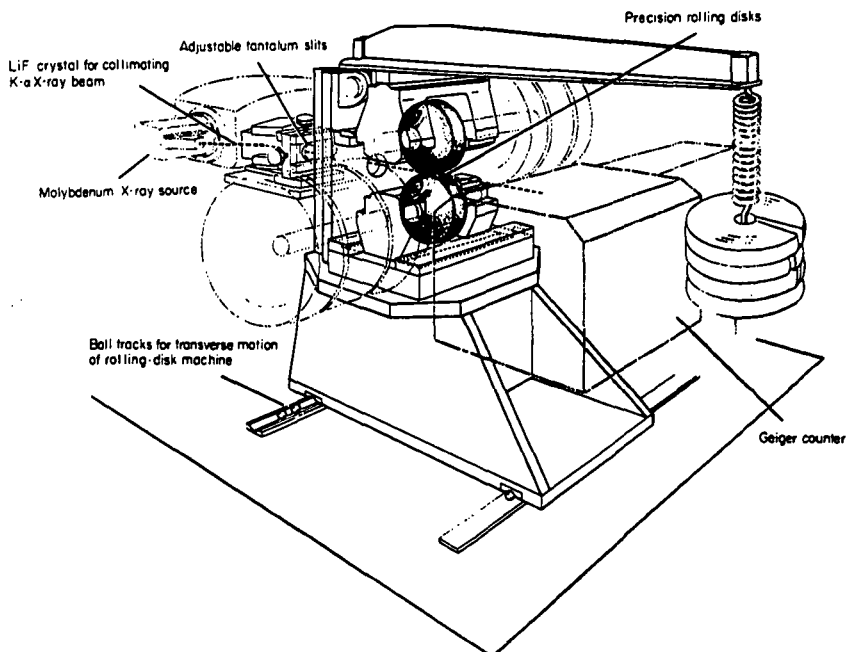


Figure 4. - Sketch of precision rolling-disk machine and X-ray system for rolling-contact-lubrication experiments (ref. 4).

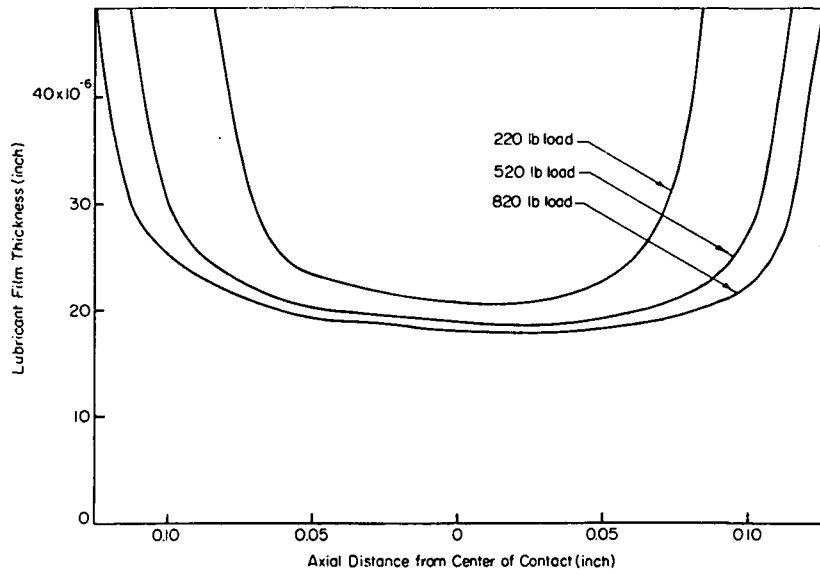


Figure 5. - Effect of load on film shape between rollers. 15 cs white mineral oil (128° F roller temperature), 2600 fpm rolling speed, smooth curves have been drawn through profile traces (ref. 4).

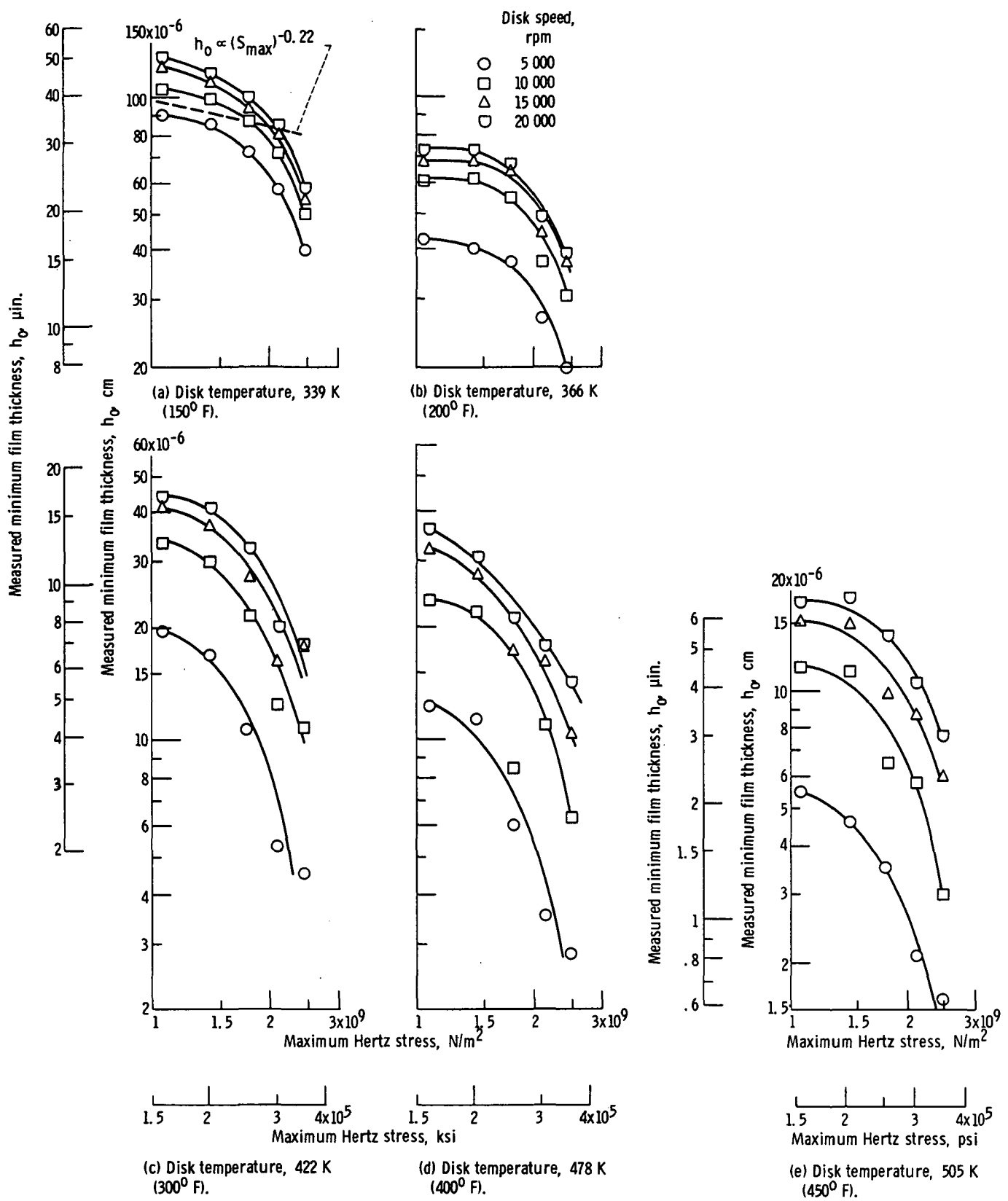


Figure 6. - Effect of maximum Hertz stress on measured minimum film thickness. Crowned-cone disks; synthetic paraffinic oil.

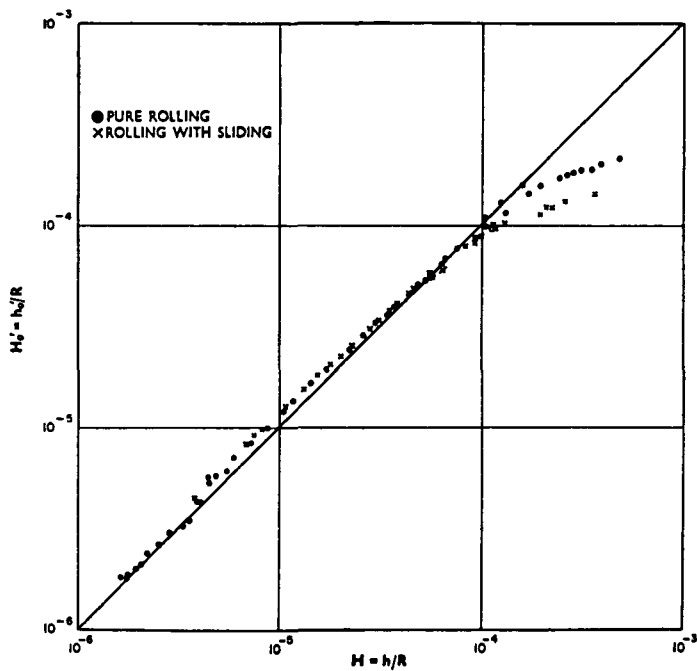


Figure 7. - Lubricant B: comparison of measured non-dimensional oil-film thickness $H'_0 = h'_0/R$ with predicted values $H = h/R$ (ref. 7).

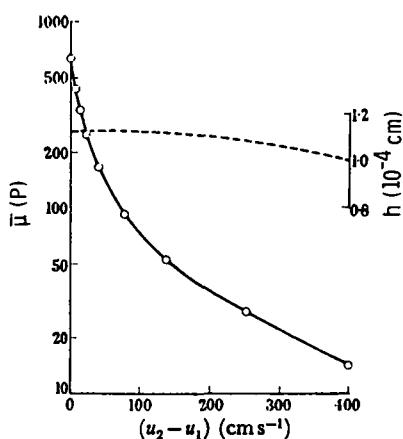


Figure 8. - The effective oil viscosity within the pressure zone ($\bar{\mu}$) as a function of sliding speed. Load $7.4 \times 10^7 \text{ dyn cm}^{-1}$; —○—, $\bar{\mu}$ (logarithmic scale); ---, h (linear scale) (ref. 6).

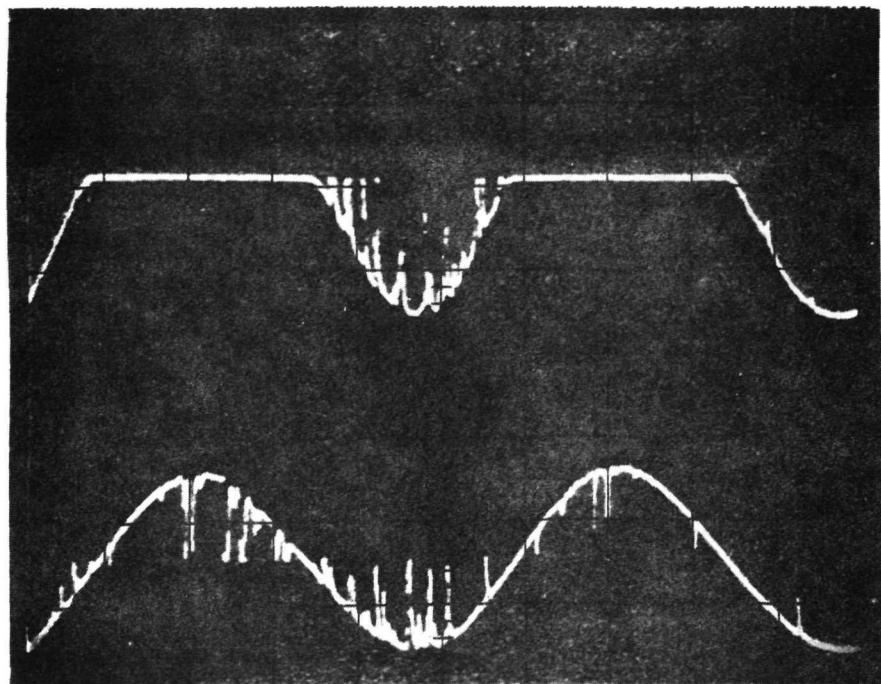


Figure 9. - Photo of 400 hertz trace of conductivity method of EHD film measurement $h/\sigma \approx 3.5$.

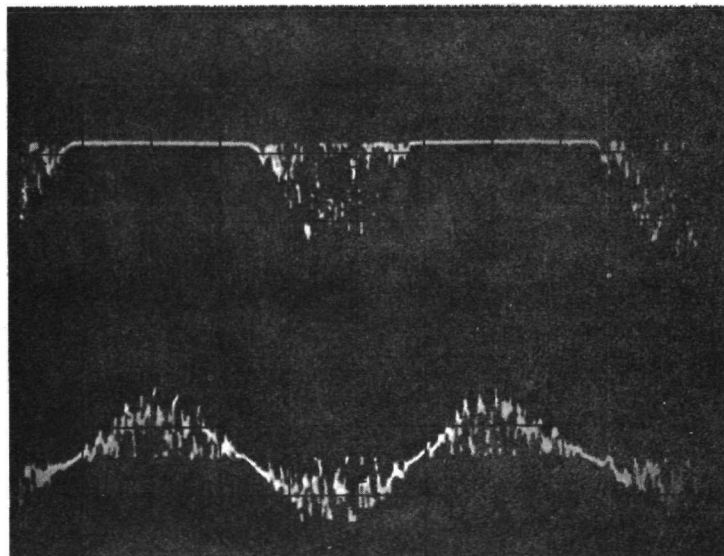


Figure 10. - Photo of 400 hertz trace of conductivity
of EHD film measurement $h/\sigma \approx 2.5$.

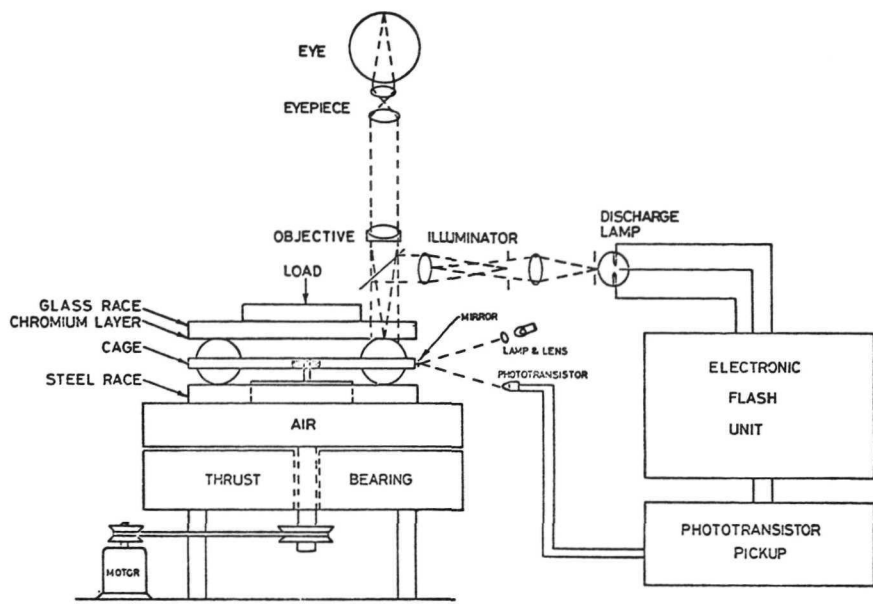


Figure 11. - Schematic diagram of optical EHD apparatus (ref. 3).

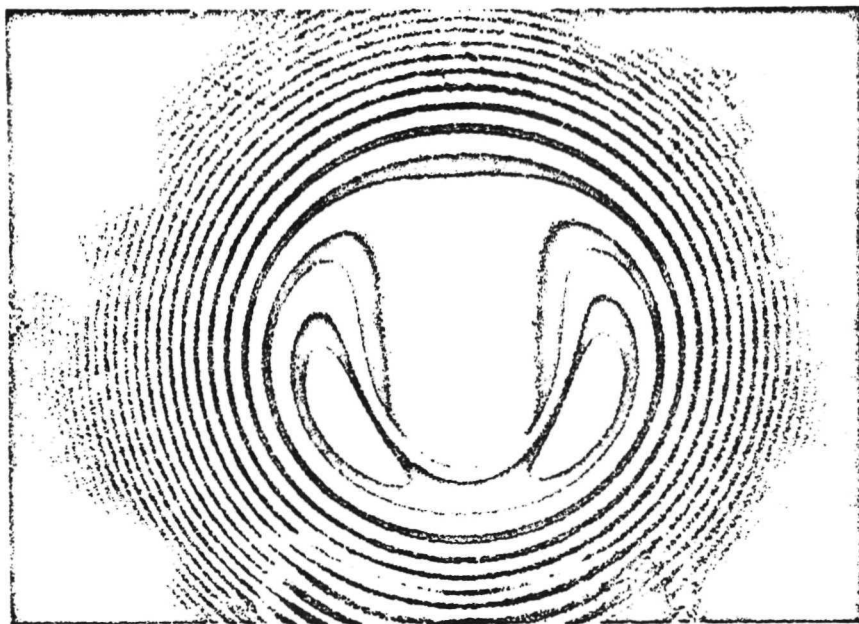


Figure 12. - Photo of optical EHD image as seen through eyepiece (ref. 3).

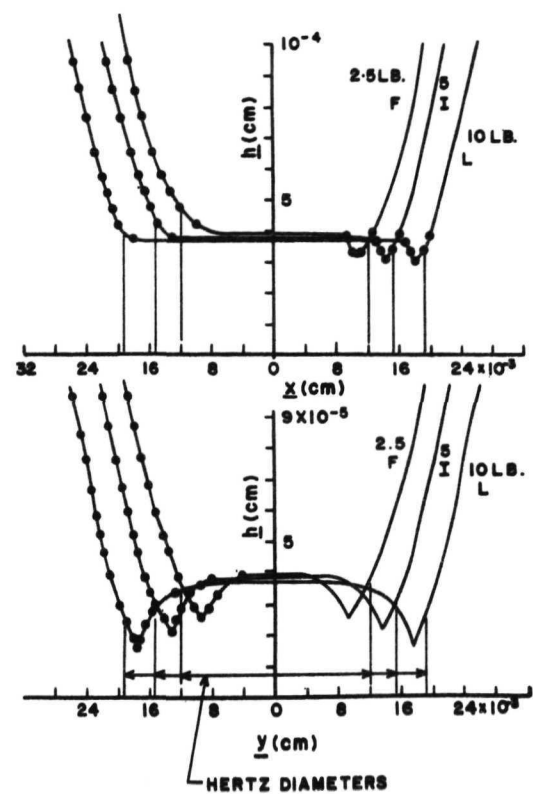


Figure 13. - Oil film profiles at different loads (ref. 3).

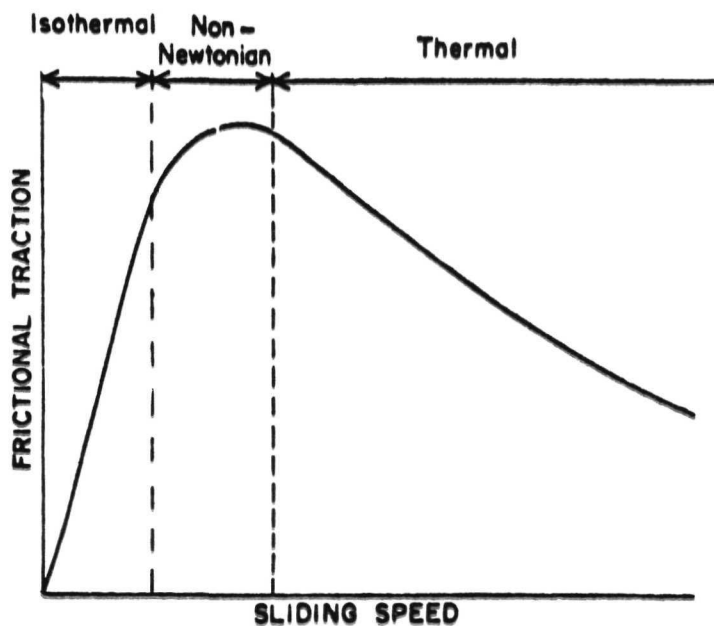


Figure 14. - Plot of friction against sliding speed (ref. 10).

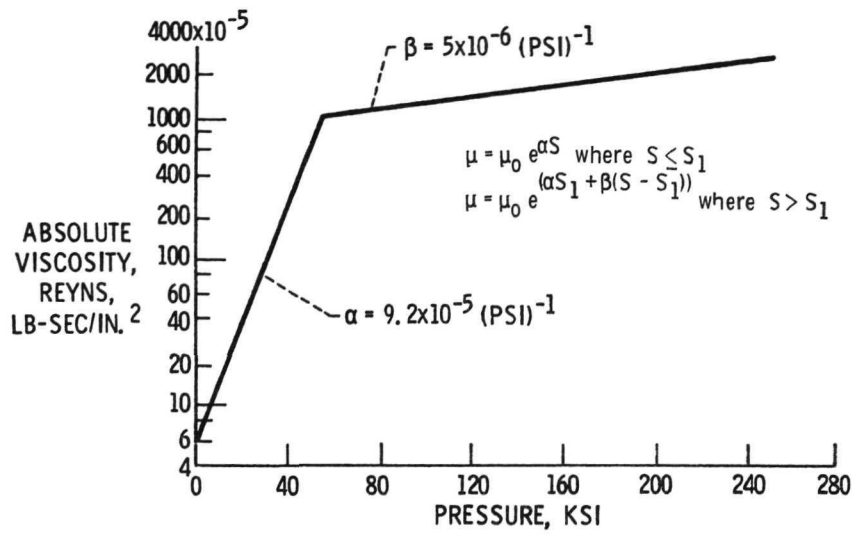


Figure 15. - Theoretical pressure-viscosity relation for synthetic paraffinic oil at 83° F (ref. 11).

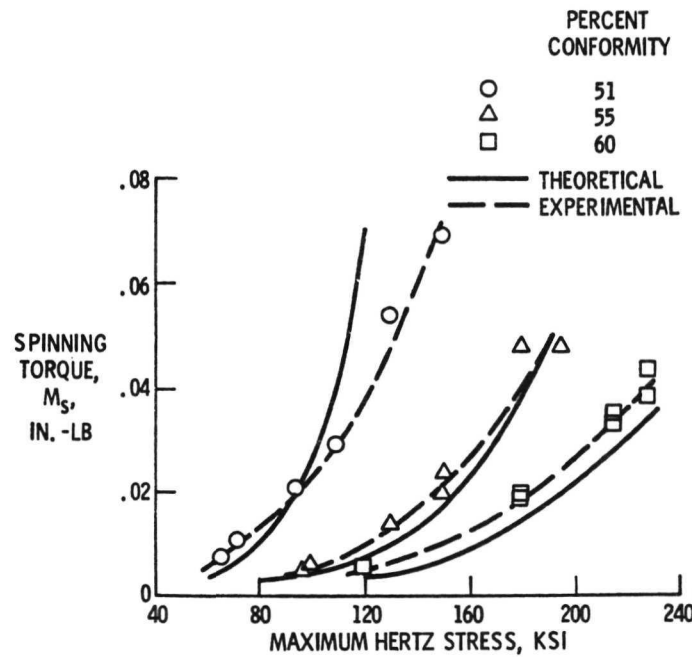


Figure 16. - Spinning torque as a function of maximum Hertz stress. Ball-oil conformity, 51, 55, and 60 percent; lubricant, synthetic paraffinic oil; pinning speed, 1050 rpm; room temperature (no heat added) (ref. 11).

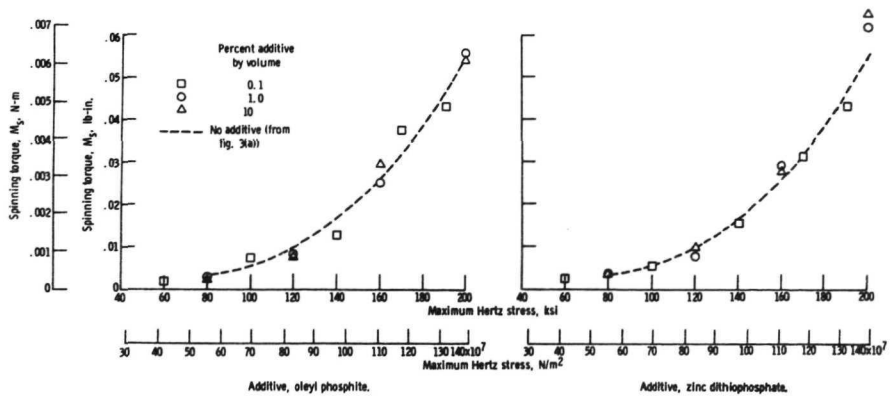


Figure 17. - Spinning torque as a function of maximum Hertz stress for synthetic paraffinic lubricant with several additives (ref. 12).

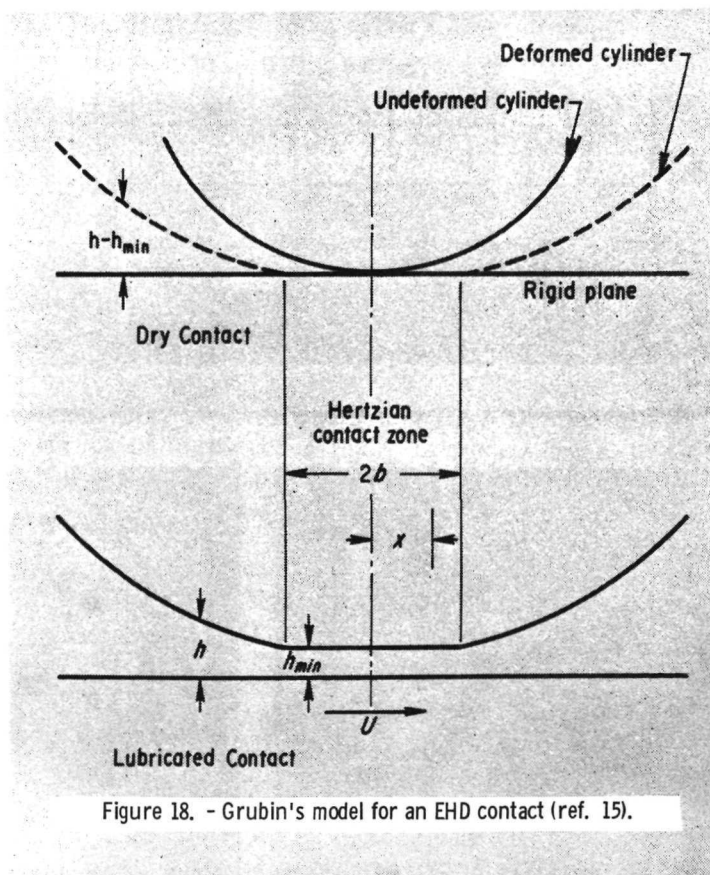


Figure 18. - Grubin's model for an EHD contact (ref. 15).

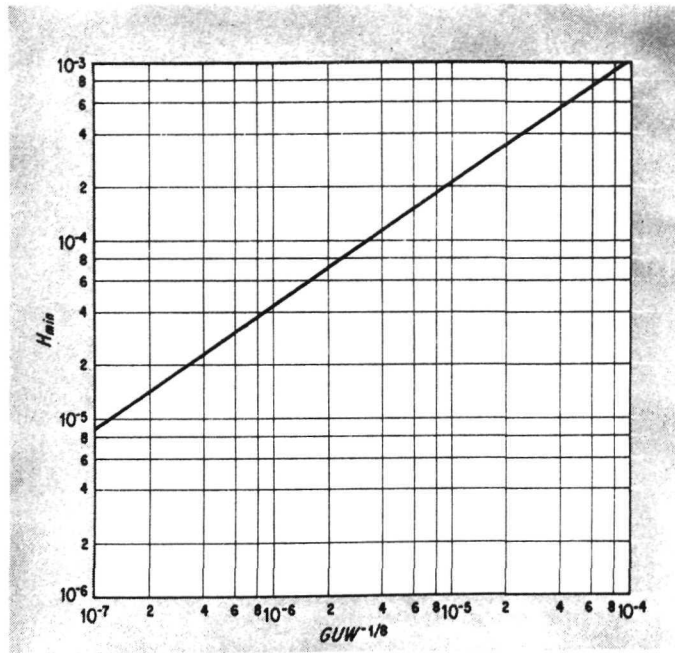


Figure 19. - Dimensionless film thickness parameter as a function of EHD parameters (ref. 14).

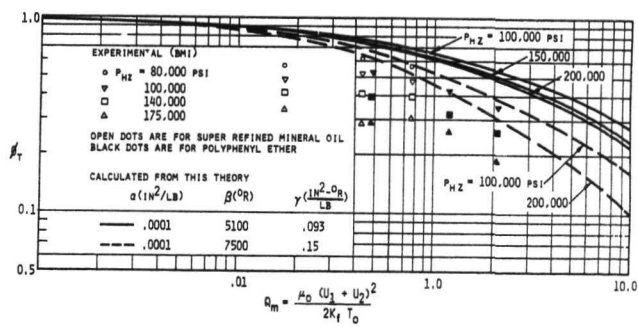


Figure 20. - Comparison of φ_t with experimental data (ref. 8).

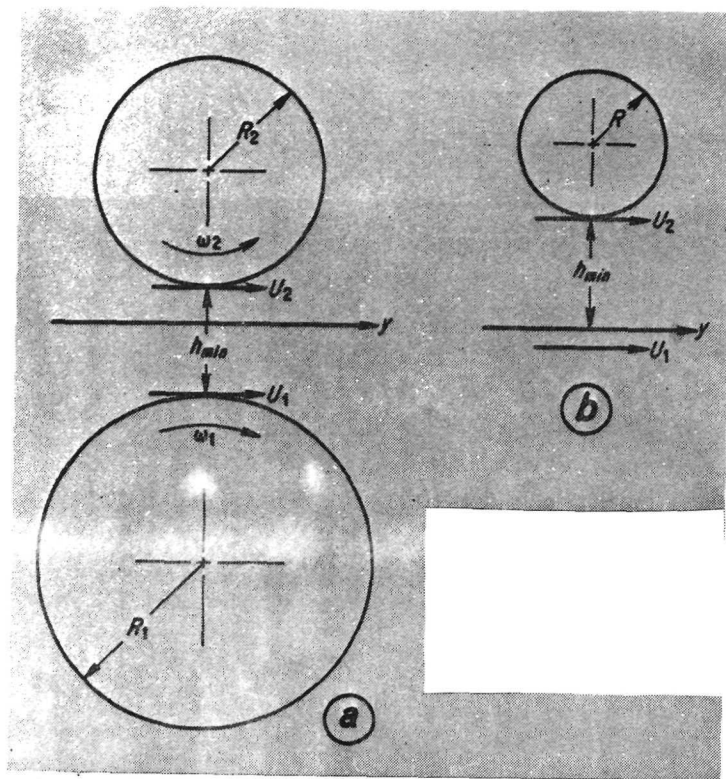


Figure 21. - Relationship between two cylinders with a lubricant film between them, a, and model of an equivalent cylinder, b (ref. 16).

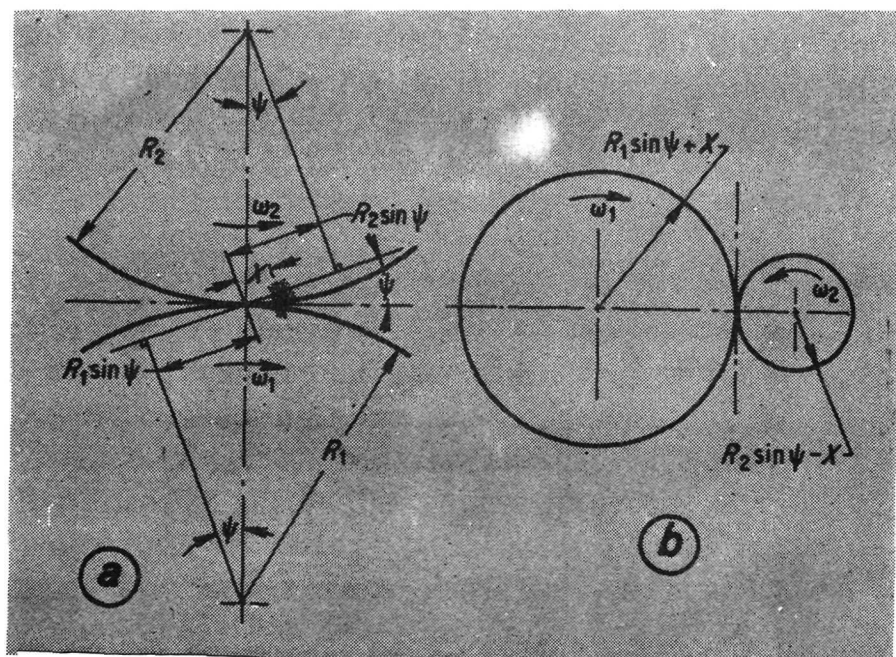


Figure 22. - Involute gears in contact, a, and equivalent cylinders, b (ref. 16).

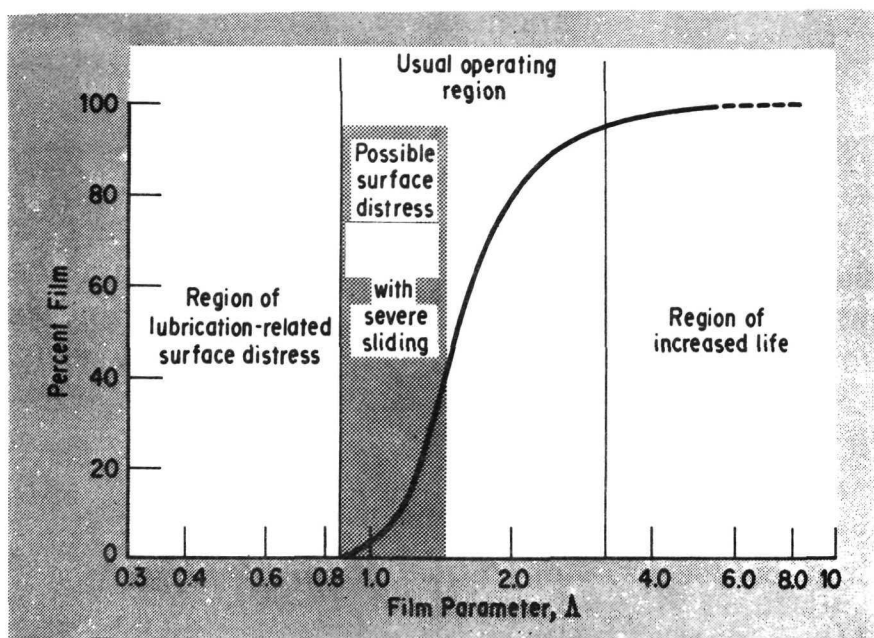


Figure 23. - Percent film as a function of film parameter (ref. 14).

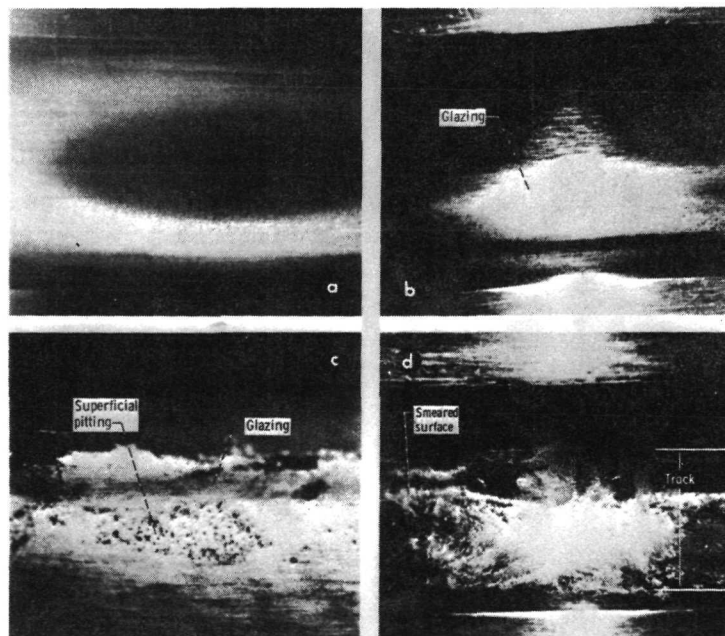


Figure 24. - Effect of EHD lubrication on surface damage to bearing races. Full EHD film results in normal race appearance, a. Marginal EHD film results in race glazing, b; glazing and superficial pitting, c; and gross plastic deformation or smearing, d.

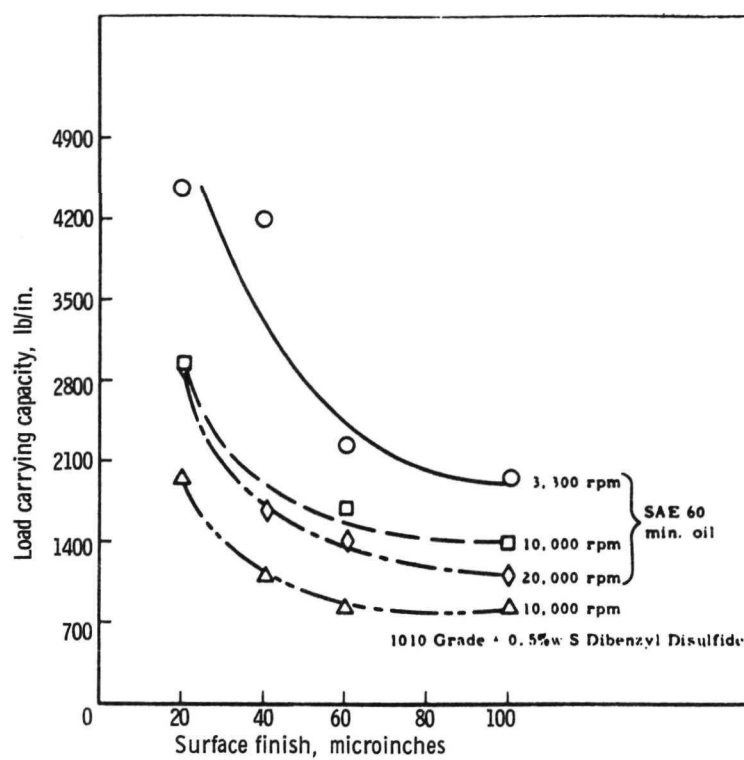


Figure 25. - Load carrying capacity versus surface finish (ref. 17).
 $DP = 6; N_1 = 17; N_2 = 19.$

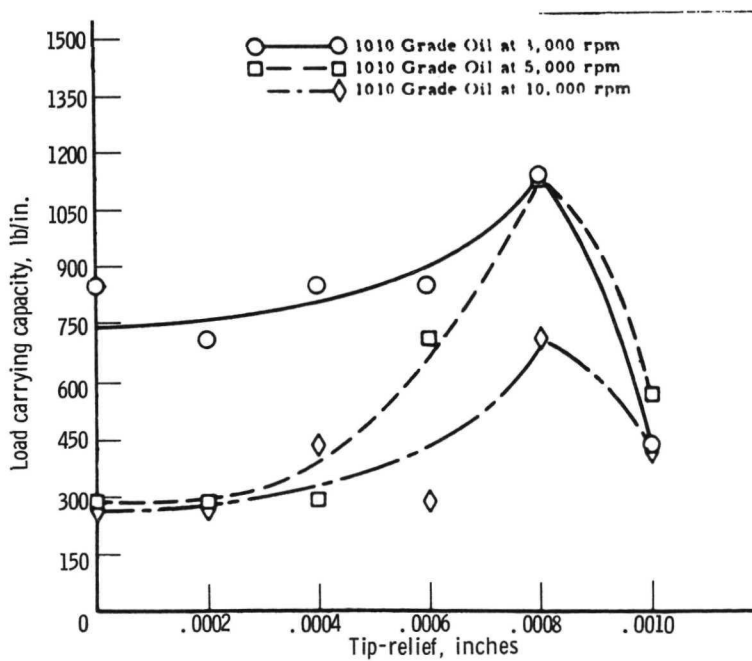


Figure 26. - Effect of tip-relief on load carrying capacity (ref. 17).
 $DP = 6; N_1 = 17; N_2 = 19.$

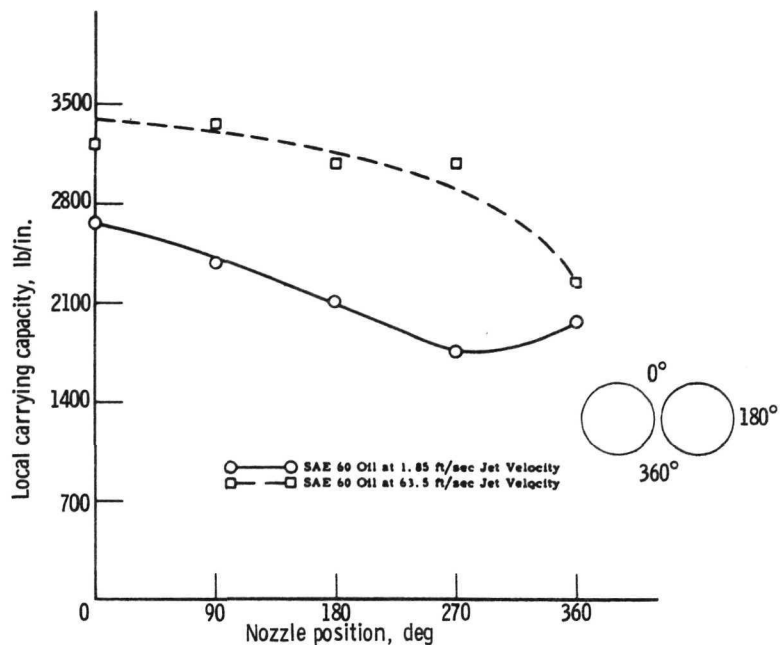


Figure 27. - Effect of jet velocity and point of application on load carrying capacity (ref. 17). $DP = C$; $N_1 = 17$; $N_2 = 19$.

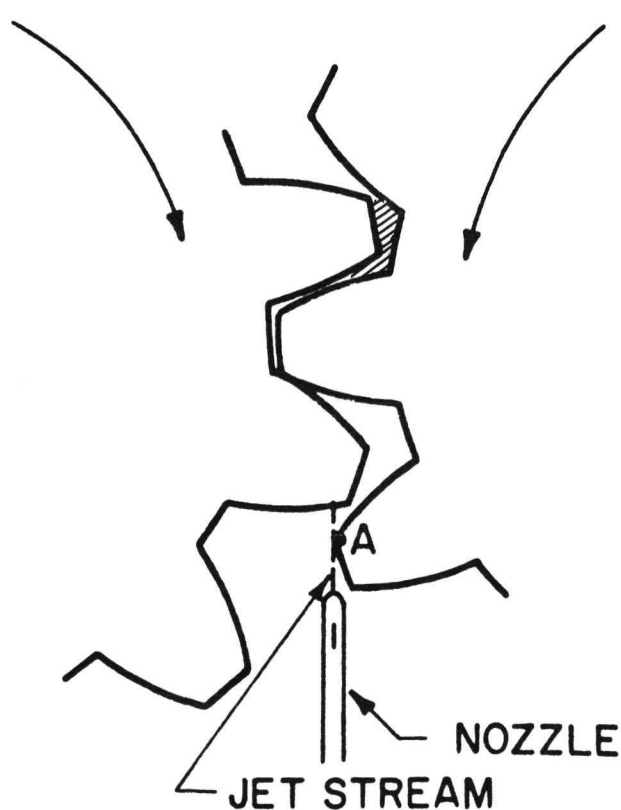


Figure 28. - Schematic of vertically oriented jet showing position for maximum oil penetration (ref. 19).

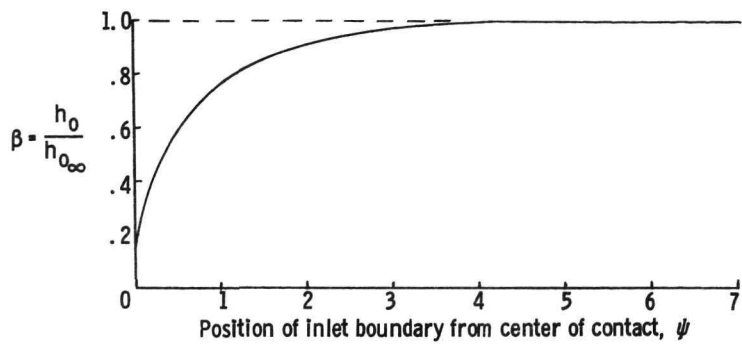


Figure 29. - The influence of the position of the inlet boundary ψ on the central film thickness β (ref. 20).

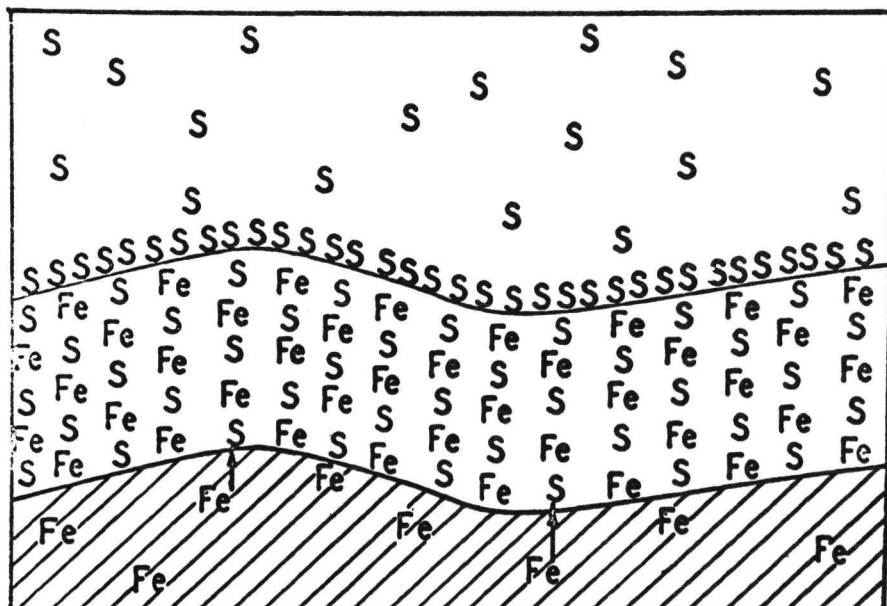


Figure 30. - Schematic representation of an inorganic film formed by reaction of sulfur with iron to form iron sulfide (ref. 21).

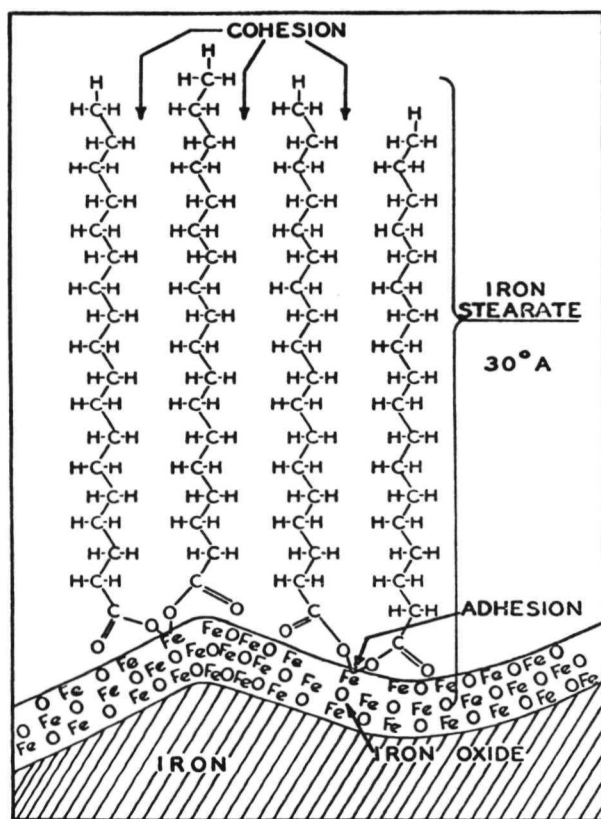


Figure 31. - Schematic diagram representing the chemisorption of stearic acid on an iron surface to form a monolayer of iron stearate, a soap (ref. 21).

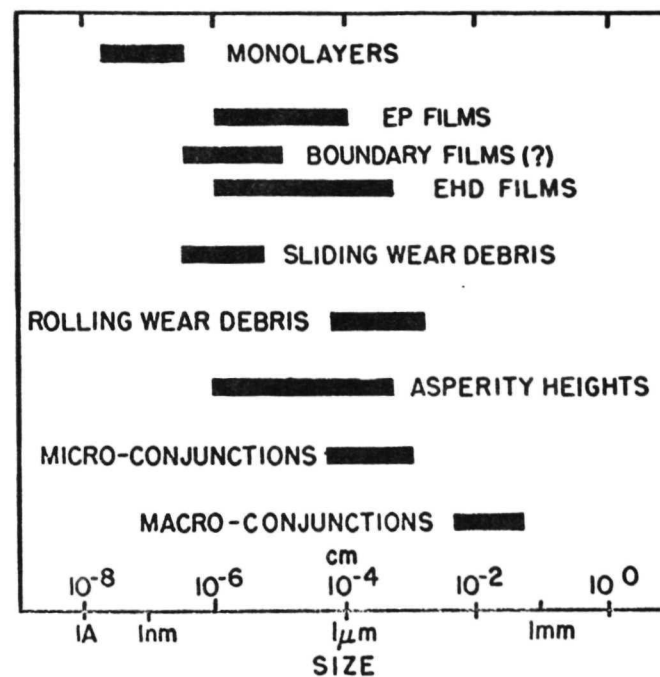


Figure 32. - Sizes pertinent to concentrated conjunction lubrication (ref. 22).

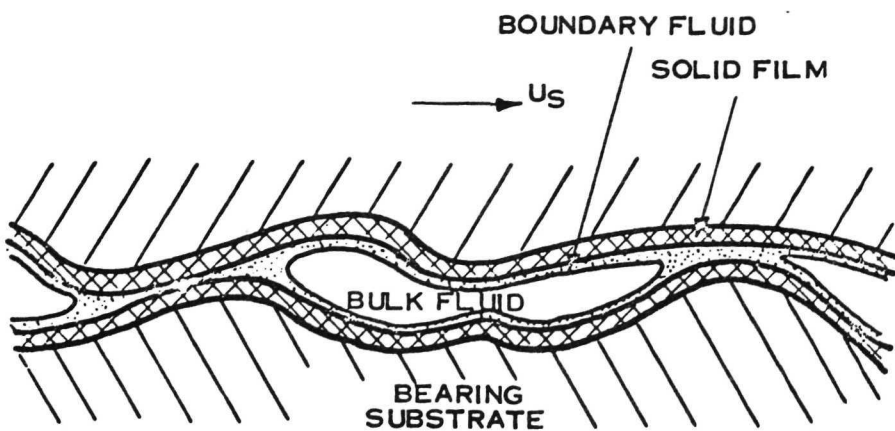


Figure 33. - Generalized MICRO-EHD model (ref. 23).

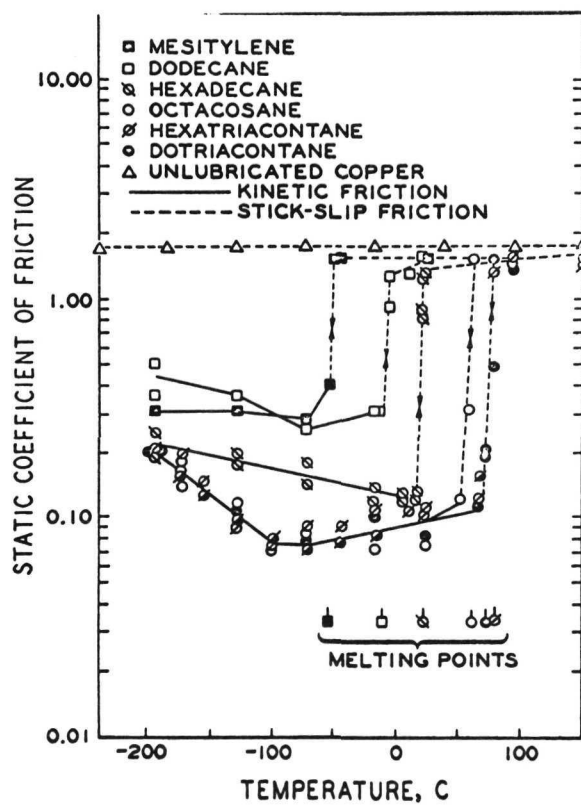


Figure 34. - Variation in friction with temperature for copper pairs lubricated with hydrocarbons in dry helium (ref. 21).

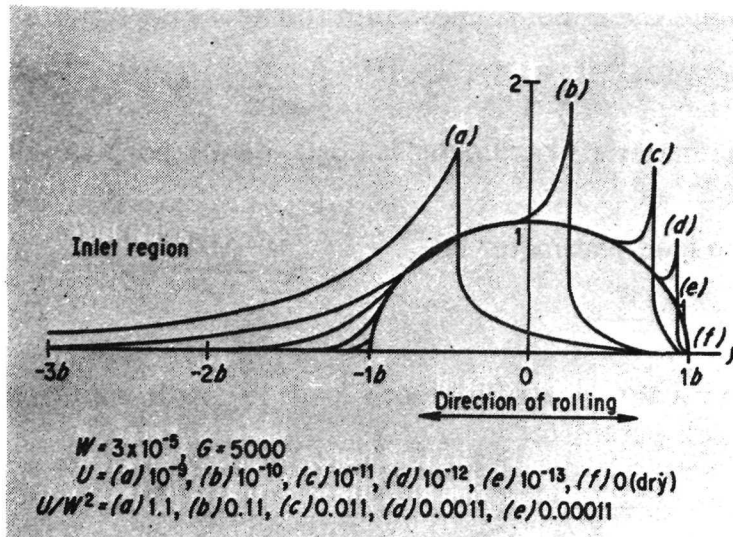


Figure 35. - Theoretical pressure distributions between lubricated rolling cylinders. As velocity increases, pressure spike shifts toward leading edge of contact (ref. 29).

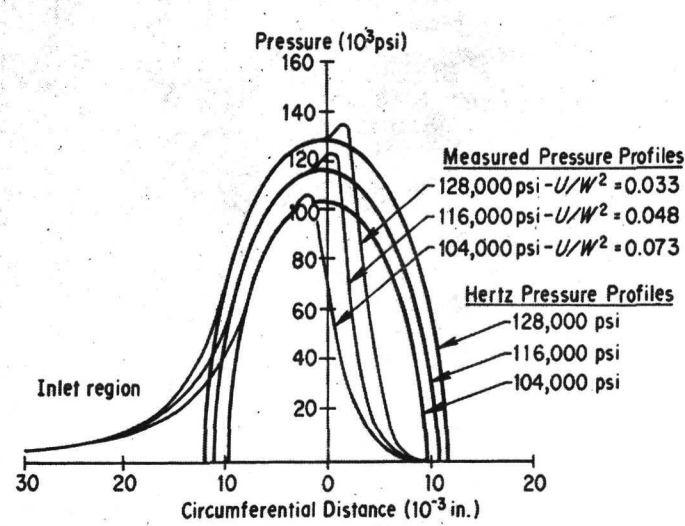


Figure 36. - Comparison of calculated Hertz pressure profiles and measured profiles between cylindrical discs with polyphenyl ether lubricant (ref. 29).

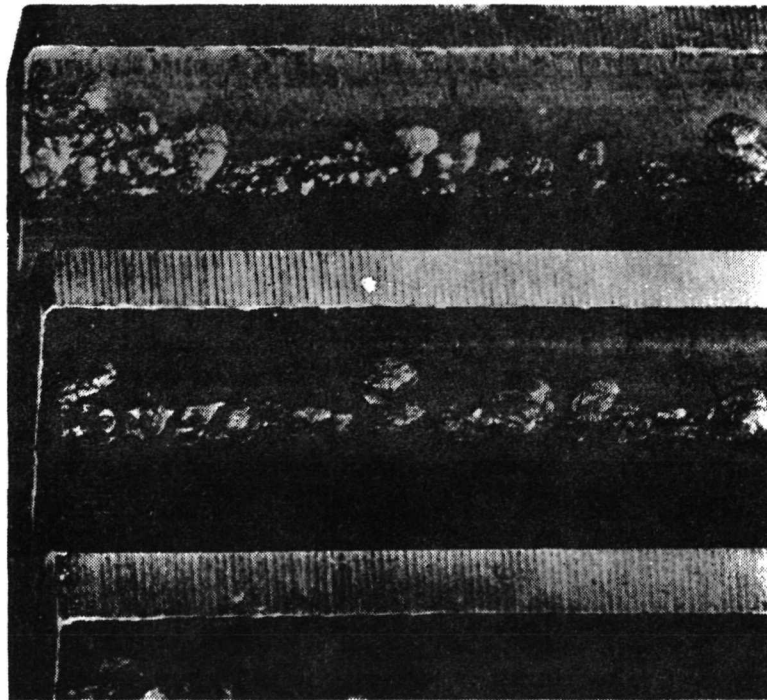


Figure 37. - Destructive pitting: Heavy pitting has taken place, predominantly in the dedendum region (ref. 30).